AFRL-RY-WP-TR-2021-0183

A CRITICAL ASSESSMENT OF ELECTRON TRANSPORT THEORY
Revised Theory of Ionized Impurity Scattering-Phase 3

Daniel L. Rode
Pendragon Associates

AUGUST 2021
Final Report

DISTRIBUTION STATEMENT A. Approved for public release. Distribution is unlimited.
See additional restrictions described on inside pages

STINFO COPY

AIR FORCE RESEARCH LABORATORY
SENSORS DIRECTORATE
WRIGHT-PATTERSON AIR FORCE BASE, OH 45433-7320
AIR FORCE MATERIEL COMMAND
UNITED STATES AIR FORCE

NOTICE AND SIGNATURE PAGE

Using Government drawings, specifications, or other data included in this document for any purpose other than Government procurement does not in any way obligate the U.S. Government. The fact that the Government formulated or supplied the drawings, specifications, or other data does not license the holder or any other person or corporation; or convey any rights or permission to manufacture, use, or sell any patented invention that may relate to them.

This report was cleared for public release by the USAF 88th Air Base Wing (88 ABW) Public Affairs Office (PAO) and is available to the general public, including foreign nationals. Copies may be obtained from the Defense Technical Information Center (DTIC) (http://www.dtic.mil).

AFRL-RY-WP-TR-2021-0183 HAS BEEN REVIEWED AND IS APPROVED FOR PUBLICATION IN ACCORDANCE WITH ASSIGNED DISTRIBUTION STATEMENT.

*//Signature//

JOHN S. CETNAR
Program Manager
Electronic Devices Branch
Aerospace Components & Subsystems Division

*//Signature//

ROSS W. DETTMER, Chief
Electronic Devices Branch
Aerospace Components & Subsystems

*//Signature//

LESTER C. LONG, Lt Col, USAF
Deputy
Aerospace Components & Subsystems Division
Sensors Directorate

This report is published in the interest of scientific and technical information exchange, and its publication does not constitute the Government's approval or disapproval of its ideas or findings.

*Disseminated copies will show "//Signature//" stamped or typed above the signature blocks.

<table>
<tr><td colspan="6">REPORT DOCUMENTATION PAGE</td><td colspan="2">Form Approved
OMB No. 0704-0188</td></tr>
<tr><td colspan="8">The public reporting burden for this collection of information is estimated to average 1 hour per response, including the time for reviewing instructions, searching existing data sources, searching existing data sources, gathering and maintaining the data needed, and completing and reviewing the collection of information. Send comments regarding this burden estimate or any other aspect of this collection of information, including suggestions for reducing this burden, to Department of Defense, Washington Headquarters Services, Directorate for Information Operations and Reports (0704-0188), 1215 Jefferson Davis Highway, Suite 1204, Arlington, VA 22202-4302. Respondents should be aware that notwithstanding any other provision of law, no person shall be subject to any penalty for failing to comply with a collection of information if it does not display a currently valid OMB control number. PLEASE DO NOT RETURN YOUR FORM TO THE ABOVE ADDRESS.</td></tr>
<tr><td colspan="3">1. REPORT DATE (DD-MM-YY)
August 2021</td><td colspan="3">2. REPORT TYPE
Final</td><td colspan="2">3. DATES COVERED (From - To)
1 February 2020 – 1 February 2020</td></tr>
<tr><td colspan="6" rowspan="3">4. TITLE AND SUBTITLE
A CRITICAL ASSESSMENT OF ELECTRON TRANSPORT THEORY
Revised Theory of Ionized Impurity Scattering-Phase 3</td><td colspan="2">5a. CONTRACT NUMBER
FA9550-20RXCOR046-RY</td></tr>
<tr><td colspan="2">5b. GRANT NUMBER</td></tr>
<tr><td colspan="2">5c. PROGRAM ELEMENT NUMBER
N/A</td></tr>
<tr><td colspan="6" rowspan="3">6. AUTHOR(S)
Daniel L. Rode</td><td colspan="2">5d. PROJECT NUMBER
N/A</td></tr>
<tr><td colspan="2">5e. TASK NUMBER
N/A</td></tr>
<tr><td colspan="2">5f. WORK UNIT NUMBER
N/A</td></tr>
<tr><td colspan="6">7. PERFORMING ORGANIZATION NAME(S) AND ADDRESS(ES)
Pendragon Associates
16400 Collins Avenue, Unit 2846
Sunny Isles Beach, Florida 33160</td><td colspan="2">8. PERFORMING ORGANIZATION REPORT NUMBER</td></tr>
<tr><td colspan="6" rowspan="2">9. SPONSORING/MONITORING AGENCY NAME(S) AND ADDRESS(ES)
Air Force Research Laboratory
Sensors Directorate
Wright-Patterson Air Force Base, OH 45433-7320
Air Force Materiel Command
United States Air Force

Air Force Office of Scientific Research Public Affairs (AFOSR)
875 North Randolph Street,
Suite 325, Room 3112
Arlington, VA 22203</td><td colspan="2">10. SPONSORING/MONITORING AGENCY ACRONYM(S)
AFRL/RYDD</td></tr>
<tr><td colspan="2">11. SPONSORING/MONITORING AGENCY REPORT NUMBER(S)
AFRL-RY-WP-TR-2021-0183</td></tr>
<tr><td colspan="8">12. DISTRIBUTION/AVAILABILITY STATEMENT
DISTRIBUTION STATEMENT A. Approved for public release. Distribution is unlimited.</td></tr>
<tr><td colspan="8">13. SUPPLEMENTARY NOTES
PAO case number AFRL-2021-0818, Clearance Date 11 March 2021. Report contains color.</td></tr>
<tr><td colspan="8">14. ABSTRACT
In Phases 1 and 2 of this work, it was shown that the widely used theory of electron transport based on the treatments of ionized-impurity scattering by Brooks & Herring and by Falicov & Cuevas cannot be relied upon for GaAs. Alternatively, the revised theory given in Phase 2 shows agreement with experiments on GaAs within a few percent, which is consistent with the current state of the experimental art. The object of the present Phase 3 work is to extend these considerations to ZnO and to GaN. The results from the present work appears to confirm the use of the revised theory of ionized-impurity scattering. A considerable revision of the calculations of electron transport theory is thus implied.</td></tr>
<tr><td colspan="8">15. SUBJECT TERMS
degeneracy, electron mobility, electronic transport, semiconductor(s)</td></tr>
<tr><td colspan="3">16. SECURITY CLASSIFICATION OF:</td><td rowspan="2">17. LIMITATION OF ABSTRACT:
SAR</td><td rowspan="2">8. NUMBER OF PAGES
29</td><td colspan="3" rowspan="2">19a. NAME OF RESPONSIBLE PERSON (Monitor)
John Cetnar
19b. TELEPHONE NUMBER (Include Area Code)
N/A</td></tr>
<tr><td>a. REPORT
Unclassified</td><td>b. ABSTRACT
Unclassified</td><td>c. THIS PAGE
Unclassified</td></tr>
</table>

Standard Form 298 (Rev. 8-98)
Prescribed by ANSI Std. Z39-18

Table of Contents

Section **Page**

1 PHASE 3: CRITICAL ASSESSMENT OF ELECTRON TRANSPORT THEORY-REVISED THEORY OF IONIZED-IMPURITY SCATTERING........ 1
1.1 Introduction........ 1
1.2 ZnO Material Parameters........ 1
1.3 Electron Mobility of Degenerate ZnO........ 4
1.4 GaN Material Parameters........ 7
1.5 GaN Carrier Freeze-Out........ 8
1.6 GaN Electron Mobility........ 12
1.7 Conclusions and Recommendations........ 18
2 ACKNOWLEDGMENTS........ 20
APPENDIX: CARRIER FREEZE-OUT........ 21
3 REFERENCES........ 23
LIST OF SYMBOLS, ABBREVIATIONS, AND ACRONYMS........ 24

DISTRIBUTION STATEMENT A. Approved for public release. Distribution is unlimited.

List of Figures

Figure **Page**

Figure 1: Electron Hall Mobility of ZnO Over the 40 to 987K Temperature Range[9] 2
Figure 2: Electron Mobility of ZnO Over the 550 to 987K Temperature Range 3
Figure 3: Electron Hall Mobility of Degenerate ZnO.. 5
Figure 4: Electron Hall Mobility of Degenerate ZnO.. 6
Figure 5: Electron Hall Mobility of Degenerate ZnO.. 6
Figure 6: The upper dashed curve assumes a compensation ratio $N_a/N_d = 0$ and m*=0.318m...... 6
Figure 7: The Lower Data Points Show the Hall Electron Concentration Measured for Sample S703 at 2kG Magnetic Field 8
Figure 8: Same Data Points as Figure 7... 9
Figure 9: Same as Figure 8 10
Figure 10: The Lower Data Points show the Hall Electron Concentration Measured for Sample 1E5 at 10kG Magnetic Field.. 11
Figure 11: The Freeze-out Behavior is Described Using One Shallow Donor and One Acceptor, with Concentrations $1.17 x 10^{16}$ and $1.4 x 10^{15}$/cc and Ionization Energy 24 mV 11
Figure 12: Same as Figure 11 12
Figure 13: The Electron Hall mobility of Sample S703 is plotted, Comparing SETA Theory (curve) and Experiment (points) 13
Figure 14: The Dashed Curve, the SETA Donor and Acceptor Concentrations are $8.35 x 10^{15}$/ and $1.0 x 10^{15}$/cc 14
Figure 15: Same as Figure 14 14
Figure 16: The Electron Hall Mobility of Sample 1E5 is Plotted, Comparing SETA Theory (curve) and Experiment (points) 15
Figure 17: Electron Hall Mobility of Sample 1E5.. 16
Figure 18: Same as Figure 16 on a Logarithmic Scale 16
Figure 19: Electron Hall Mobility of Doped n-type GaN... 17
Figure 20: Same as Figure 19 18
Figure 21: Data Points by Morkoç (open circles) and Kyle (solid circles) 19

DISTRIBUTION STATEMENT A. Approved for public release. Distribution is unlimited.

1 PHASE 3: CRITICAL ASSESSMENT OF ELECTRON TRANSPORT THEORY-REVISED THEORY OF IONIZED-IMPURITY SCATTERING

By Daniel L. Rode
Pendragon Associates

"If any person choose it, he may save five or six shillings for the present, and wait five or six years longer (if I should live so long) for the opportunity of buying the same thing, probably much enlarged..." — Joseph Priestley (1775)

1.1 Introduction

In Phases 1 and 2 of this work,[1,2] it was shown that the widely used theory of electron transport based on the treatments of ionized-impurity scattering by Brooks & Herring and by Falicov & Cuevas cannot be relied upon for GaAs. Alternatively, the revised theory given in Phase 2 shows agreement with experiments on GaAs within a few percent, which is consistent with the current state of the experimental art. The object of the present Phase 3 work is to extend these considerations to ZnO and to GaN so as to seek further confirmation of the revised theory.

Of special concern is the commonly used method of assuming dopant compensation by acceptor impurities in order to explain experimental results in terms of electron transport theory when using the Brooks-Herring theory (BH). The present Phase 3 work offers an alternative to this approach.

This final phase of the present work appears to confirm the use of the revised theory of ionized-impurity scattering referenced above. A considerable revision of the calculations of electron transport theory is thus implied.

1.2 ZnO Material Parameters

A thorough experimental Hall Effect study of degenerately doped Zinc Oxide (ZnO) (Sample G3ZO-313) has been carried out at AFRL, and the data have been made available for the analysis below.[3]

However, before setting out to analyze the experimental data, it is essential to establish a reliable set of basic material parameters to be used in the Semiconductor Electronic Transport Analysis (SETA) calculations.[4-6] These are eight in number:

1) static dielectric constant K_s
2) high-frequency dielectric constant K_∞
3) polar-optical phonon energy (or temperature) T_{po}
4) longitudinal elastic constant c_L
5) acoustic phonon deformation potential E_1
6) piezoelectric constant P_{pe}
7) effective-mass energy gap E_g
8) electron effective mass (or polaron mass) m^*

DISTRIBUTION STATEMENT A. Approved for public release. Distribution is unlimited.

All of these parameters, except the effective mass, are sufficiently accurately known to be suitable for present purposes. The effective mass, so-called here, is in fact the polaron mass, which is discussed in the literature.[5] The effective mass was estimated by Rode[6] (in the absence of direct measurement) as 0.318m; by Look *et al.*[7] as 0.34m from comparisons to mobility calculations; and from cyclotron resonance measurements by Miura and Imanaka[8] as 0.290m. These variations fall outside the desired range of ±0.01m for the present work.

Some criticism of these three numbers may be lodged as follows. The 0.318 figure by Rode is merely an estimate based on comparisons with similar semiconductors, and its accuracy is unknown. The 0.34 figure by Look *et al.* is based on transport calculations which do not include conduction band non-parabolicity and wave-function admixture, and the accuracy is likewise unknown if all these effects were to be included, as they are in the SETA work below. The cyclotron resonance work by Miura and Imanaka used very large magnetic field strengths (mega-gauss) and therefore they are confused with LO phonon resonance effects as well as band non-parabolicity. Clearly, another approach is needed.

We offer the following. Hall Effect work by Hutson[9] on n-type ZnO was carried out over the temperature range 40 to 987K. See Fig. 1. The material is low-doped and unaffected by ionized-impurity scattering above room temperature. Therefore, since all the other material parameters are known, it should be possible to accurately determine the effective (polaron) mass by comparisons between theory and experiment at the higher temperatures.

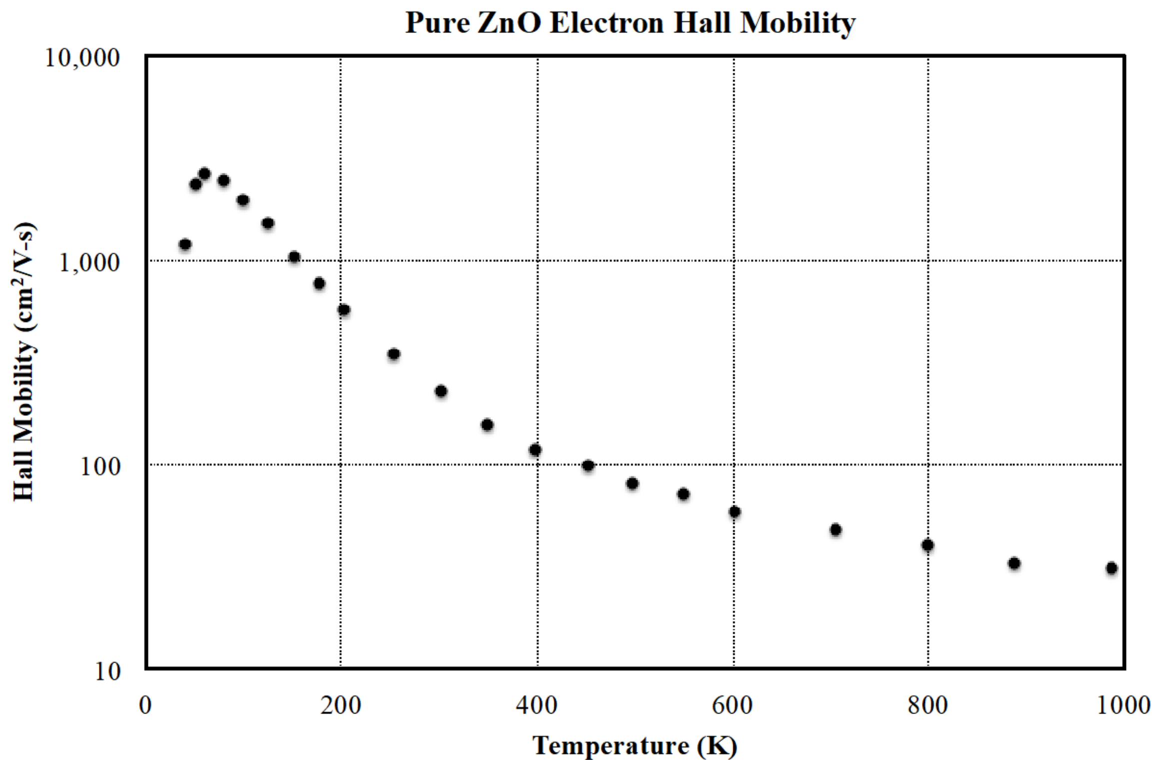

Figure 1: Electron Hall Mobility of ZnO Over the 40 to 987K Temperature Range[9]

The magnetic field is 982 gauss.

DISTRIBUTION STATEMENT A. Approved for public release. Distribution is unlimited.

In Figure 2, a comparison between theory and experiment is shown for two different values of the effective mass: 0.34m (lower curve) and 0.32m (upper curve). The theoretical SETA calculation includes conduction band non-parabolicity and wave-function admixture. Obviously, the lower curve is in very good agreement with experiment (solid points) over the temperature range 550 to 987K, indicating the effective mass may be taken to be 0.34m *in the neighborhood of 750K*.

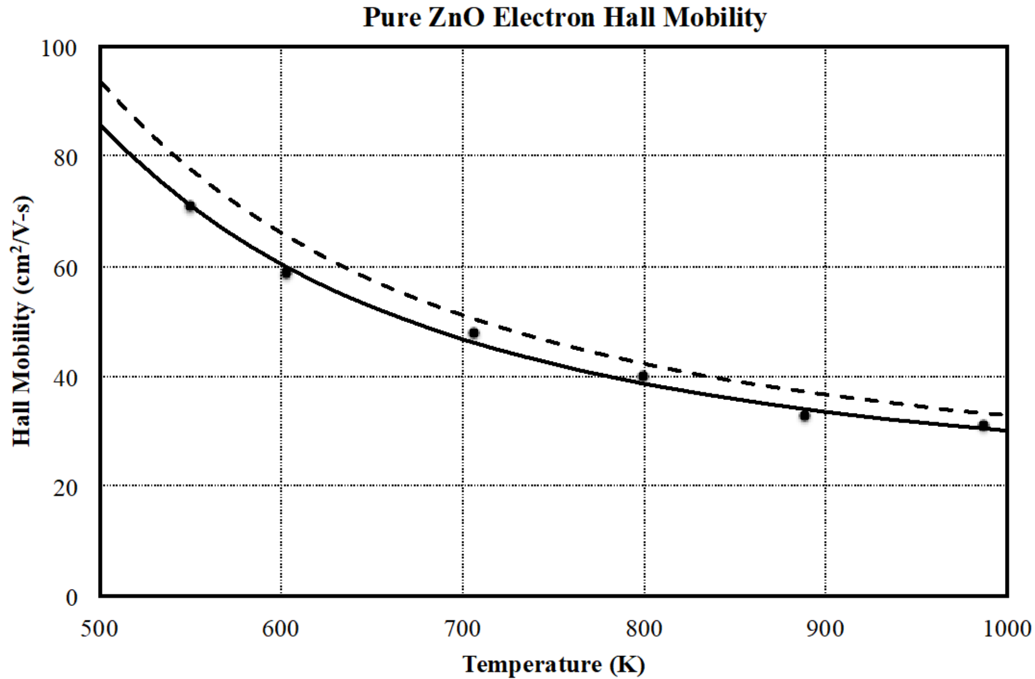

Figure 2: Electron Mobility of ZnO Over the 550 to 987K Temperature Range
Effective mass is taken to be 0.34m and 0.32m for the lower and upper curves.

However, the effective mass is needed for T=300K. The temperature dependence can be estimated in two ways: energy-gap scaling according to the Kane band theory,[6] or comparison to similar materials. The cyclotron resonance effective mass of CdS has been found to vary from 0.151m to 0.147m from 150K to 300K.[8] Applying this same variation to ZnO implies an effective mass change of 8.2% from 300K to 750K, or 0.37m at 300K. But this must be an over-estimate of the change of effective mass because ZnO is not entirely equivalent to CdS, and because phonon resonance effects are operative for the mega-gauss magnetic fields used in the cyclotron resonance measurements.[8] Therefore, the 0.37m estimate seems to be an upper bound.

Using energy-gap scaling based on the energy gap of ZnO versus temperature reported by Hauschild et al.[10] gives an effective mass change of 4.8% from 300K to 750K, or 0.356m at 300K if the effective mass is 0.34m at 750K. For degenerately doped ZnO there will be further bandgap shrinkage due to heavy doping, so the effective mass may be further slightly reduced. Lastly, the temperature dependence of the optical phonon energy affects the polaron coupling strength, and this also has been ignored. Accordingly, we take m*=0.35m for T=300K (instead of 0.356m), which is comfortably within the ±0.01m tolerance desired, although 0.356m is so

DISTRIBUTION STATEMENT A. Approved for public release. Distribution is unlimited.

nearby that the calculations would hardly show any difference in electron Hall mobility, i.e. about 2%.

The remaining material parameters are taken from the literature. Thus, the 300K ZnO material parameters are taken to be as follows.[6]

1) static dielectric constant $K_s = 8.12$
2) optical dielectric constant $K_\infty = 3.72$
3) polar-optical phonon temperature $T_{po} = 837K$
4) longitudinal elastic constant $c_L = 207GPa$
5) acoustic phonon deformation potential $E_1 = 3.8eV$
6) piezoelectric constant $P_{pe} = 0.21$
7) effective-mass energy gap $E_g = 3.43eV$
8) electron mass (polaron mass) $m^* = 0.35m$

These material parameters are used for the SETA calculations given in the next section.

1.3 Electron Mobility of Degenerate ZnO

Electron Hall mobility data[3] for degenerately doped ZnO (Sample G3ZO-313) are shown in Figure 3 for T=20 to 320K. The theoretical calculations shown by the dashed curve are SETA calculations using the above material parameters, except that m* is set equal to 0.318m, as suggested by Rode.[6] For both the experiment and the theoretical calculations the magnetic field is 10kG. The conduction electron concentration and the donor concentration are both $8.84\text{x}10^{20}$/cc, as given by experiment. The acceptor concentration is taken to be zero, *i.e.* there is no dopant compensation by acceptors. As one can see, the theoretical curve is 10 to 12% too high.

The same electron Hall mobility data are shown repeated in Figure 4 and compared to the SETA calculation using the effective mass set equal to the presently preferred 0.35m. The agreement between theory and experiment is within the desired few percent. To show this more clearly, the same data are repeated on a larger scale in Figure 5.

It is apparent that the agreement between theory and experiment is generally within about 3% when the 300K effective mass is set equal to 0.35m, a highly satisfactory result. Equally intriguing is the fact that no acceptor compensation whatever is needed to achieve these results. Nevertheless, one wonders what effect acceptor compensation might have on the results shown in Figure 5. To this end, Figure 6 shows the results for an assumed compensation ratio $N_a/N_d = 0.1$. It appears that the compensation ratio must be quite small compared to 0.1 if not indeed essentially zero if m* = 0.35m. Also in Figure 6, the solid curve is nearly identical to that for m* = 0.318m and a compensation ratio of 0.06, which is similar to the compensation ratios reported by Look *et al.*[7]

In conclusion, for degenerately Ga-doped ZnO, it is quite possible to accurately describe the transport behavior of electrons without inferring dopant compensation by acceptors provided the

DISTRIBUTION STATEMENT A. Approved for public release. Distribution is unlimited.

revised theory of ionized-impurity scattering is used. It would be desirable to test this conclusion on other, variously doped ZnO samples, and at elevated temperature such as 750 to 1000K.

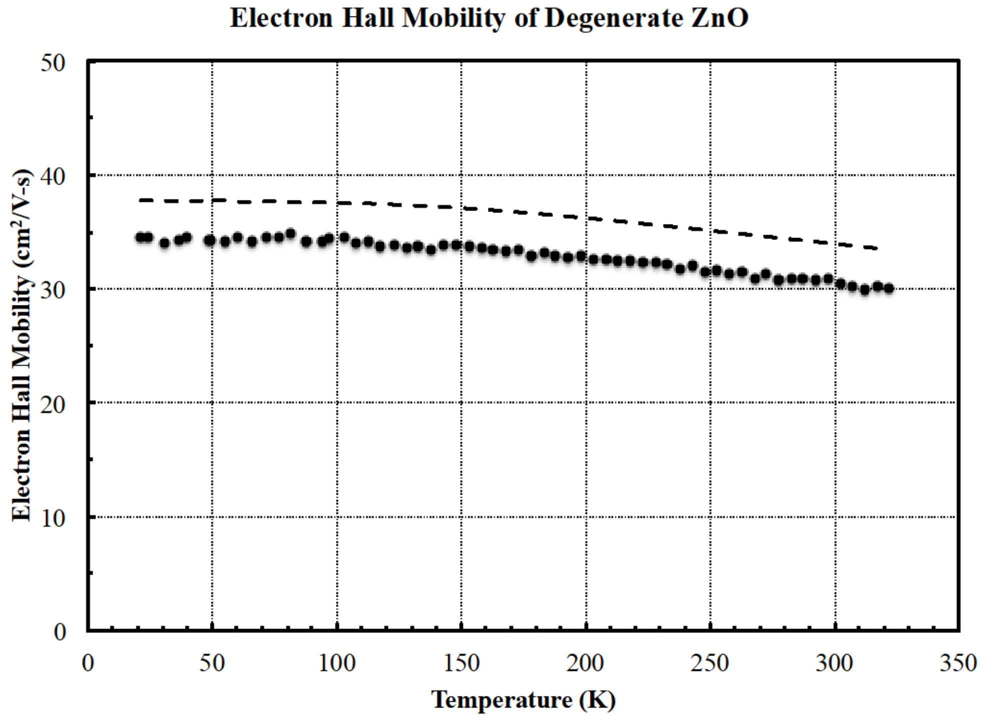

Figure 3: Electron Hall Mobility of Degenerate ZnO

Solid points are experimental. Dashed curve is the theoretical SETA calculation. Effective mass is 0.318m for the theoretical curve. The theoretical curve is 10 to 12% too high.

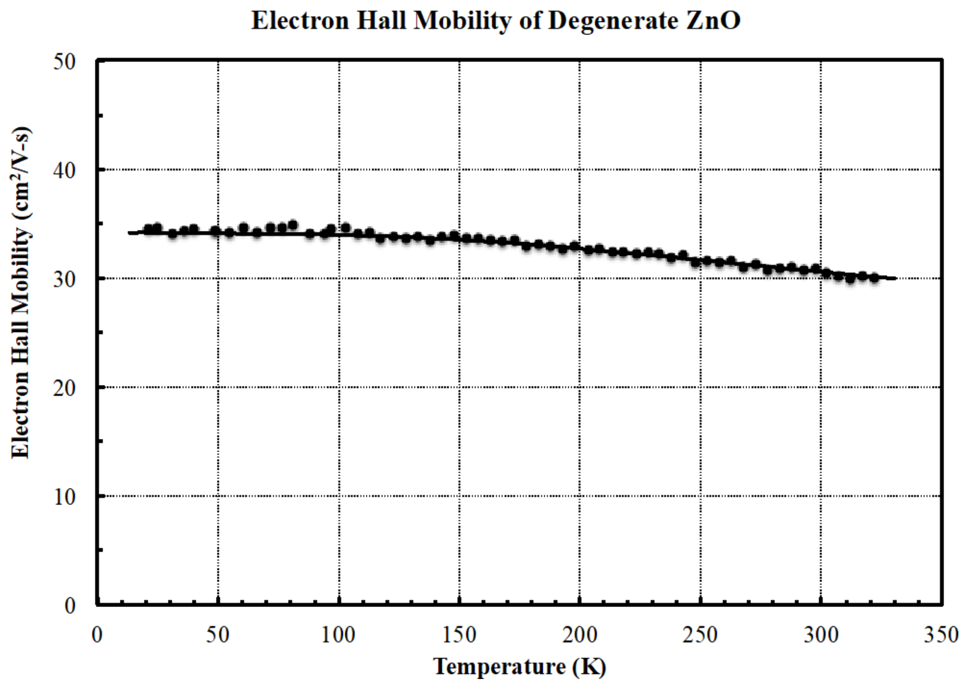

DISTRIBUTION STATEMENT A. Approved for public release. Distribution is unlimited.

Figure 4: Electron Hall Mobility of Degenerate ZnO

Solid points are experimental. The solid curve is the theoretical SETA calculation with m=0.35m.*

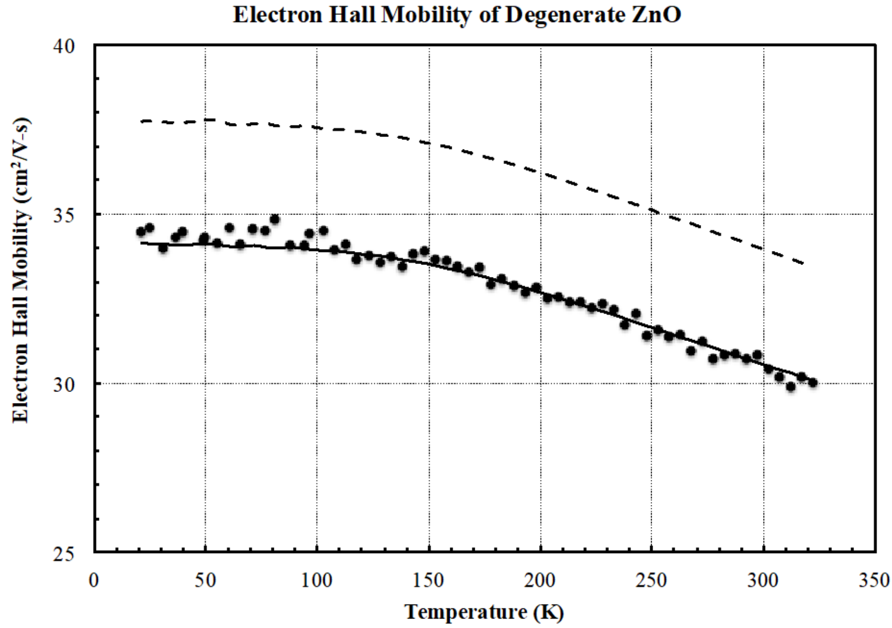

Figure 5: Electron Hall Mobility of Degenerate ZnO

Solid points are experimental. The dashed curve is the theoretical SETA calculation with m=0.318m and the solid curve is the theoretical SETA calculation with m*=0.35m.*

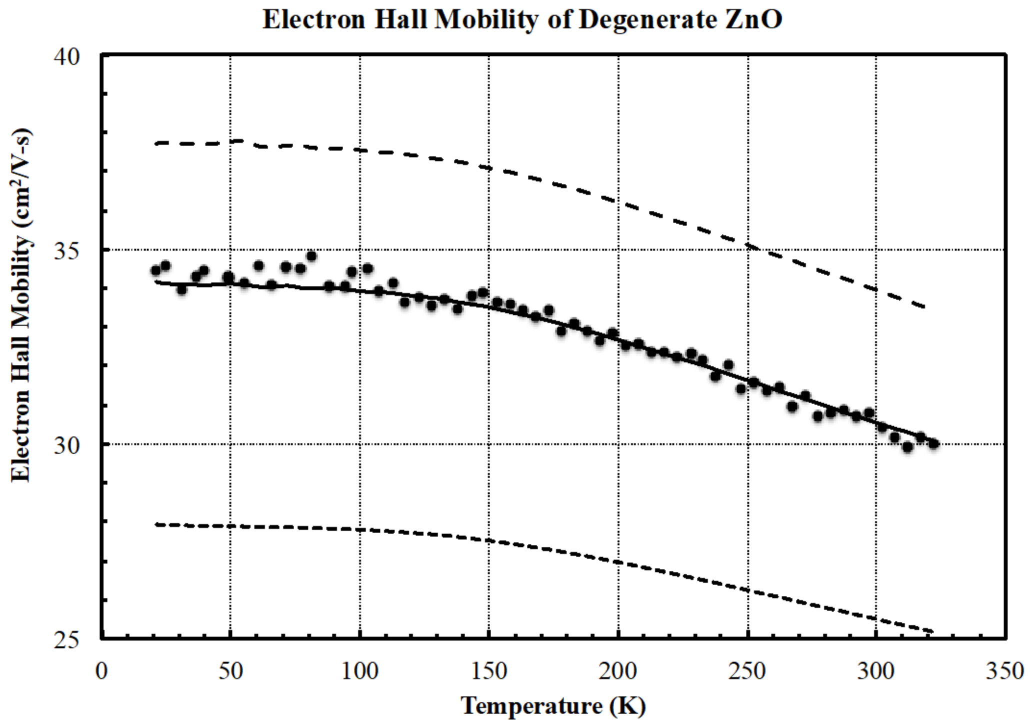

Figure 6: The upper dashed curve assumes a compensation ratio $N_a/N_d = 0$ and m*=0.318m

DISTRIBUTION STATEMENT A. Approved for public release. Distribution is unlimited.

The solid curve uses N_a/N_d = 0 and m=0.35m. The lower dashed curve uses a compensation ratio N_a/N_d = 0.1 and m*=0.35m.*

1.4 GaN Material Parameters

In order to analyze experimental Hall Effect data on GaN, it is essential to first arrive at a set of basic material parameters. Unfortunately, this area of GaN research appears to be in need of some revision. Careful measurements based on more-recently available free-standing specimens of GaN, including measurements over the 100 to 1000K temperature range, are greatly to be desired. For 300K GaN, the parameters are taken here to be as follows:

1) static dielectric constant $K_s = 10.19$
2) high-frequency dielectric constant $K_\infty = 5.35$
3) polar-optical phonon energy (or temperature) $T_{po} = 1056K$
4) longitudinal elastic constant $c_L = 372GPa$
5) acoustic phonon deformation potential $E_1 = 8.4eV$
6) piezoelectric constant $P_{pe} = 0.145$
7) effective-mass energy gap $E_g = 3.39eV$
8) electron mass (polaron mass) $m^* = 0.22m$

These parameters differ from those given by Rode.[6] Material parameters given in the literature are a hodgepodge, so some discussion of the parameters is warranted. A very comprehensive review of several nitride-semiconductors is given by Vurgaftman and Meyer, who list 428 literature references.[11] An excellent review is also given by Look and Sizelove.[12]
There is not much difficulty with the effective-mass energy gap (3.39eV) because electron mobility is not sensitive to energy gap, even considering the zincblende *vs.* wurtzite structure of GaN. The temperature and pressure dependences of the energy gap are discussed by Shan *et al.*[13] This leads to a deformation potential which seems to be an upper-bound estimate (9.2eV) because it ignores the motion of the valence band with pressure. Hence, the 8.4eV figure from Rode[6] is chosen, but this may need to be re-visited. It should be pointed out that Look and Sizelove[12] obtained a good fit between theory and experiment on electron mobility using a deformation potential of 13.5eV.

The 5.35 value for the optical (or high-frequency) dielectric constant is well-established[14,15,16,17] and is used in conjunction with the Lyddane-Sachs-Teller Relation to derive the static dielectric constant: $10.19 = 5.35 \times (734.0/531.8)^2$ using the Davydov *et al.*[18] LO and TO phonon frequencies, 734.0 and 531.8/cm. This result agrees well with the results by Park *et al.*,[17] 10.12(para) and 9.8(perp) at 300K and 10.02(para) and 9.3(perp) at 800K, at least for the "para" result, *i.e.* parallel to the c-axis of the wurtzite structure. The 734/cm LO phonon frequency of Davydov[18] *et al.* gives the 1056K LO phonon temperature.

The elastic constant, 372GPa from Polian *et al.* [19] differs significantly from Rode (265GPa) and from Davydov *et al.* (305.33GPa) but is arguably preferred by Vurgaftman and Meyer.[11] Savastenko and Shelag give 266.2GPa but this seems too small in view of later work.[20] These considerations also lead to some doubt about the piezoelectric constant (0.145 above) and, perhaps the 0.083 of Look and Sizelove[12] should be adopted. This must be left to future work.

DISTRIBUTION STATEMENT A. Approved for public release. Distribution is unlimited.

That leaves only the effective mass to be considered. Rode[6] estimated 0.218m by comparison to similar semiconductors, in the absence of experimental data. Barker and Ilegems[14] gave 0.2±0.02m. Perlin *et al.* [21] give 0.22m based on plasma frequency measurements. However, this result is affected to an unknown extent by the Hall Factor, non-parabolicity, and the dielectric constant. Look and Sizelove,[12] and Morkoç *et al.*[22] also use 0.22m, and this value is adopted here.

1.5 GaN Carrier Freeze-Out

Thanks to generous assistance from Look and Cooper[23] (AFRL), from Kyle and Speck[24] (UCSB), and from Morkoç[22,25] (VCU) who provided Hall Effect data on high-purity n-type GaN, it is possible to estimate the donor and acceptor concentrations of GaN samples using carrier freeze-out analyses, and to see if the concentrations are capable of yielding quantitative explanations of the electron mobility as a function of temperature using SETA analyses. This is the first time this has been attempted including non-parabolic conduction band and wave-function admixture.

a) AFRL Sample S703

The freeze-out curves are computed using the contraction mapping solution of the charge-balance equation set out in the Appendix: Carrier Freeze-Out. The method given in the Appendix is capable of accommodating any number of donors simultaneously. Experimental data on AFRL GaN Sample S703 are shown in Figure 7.

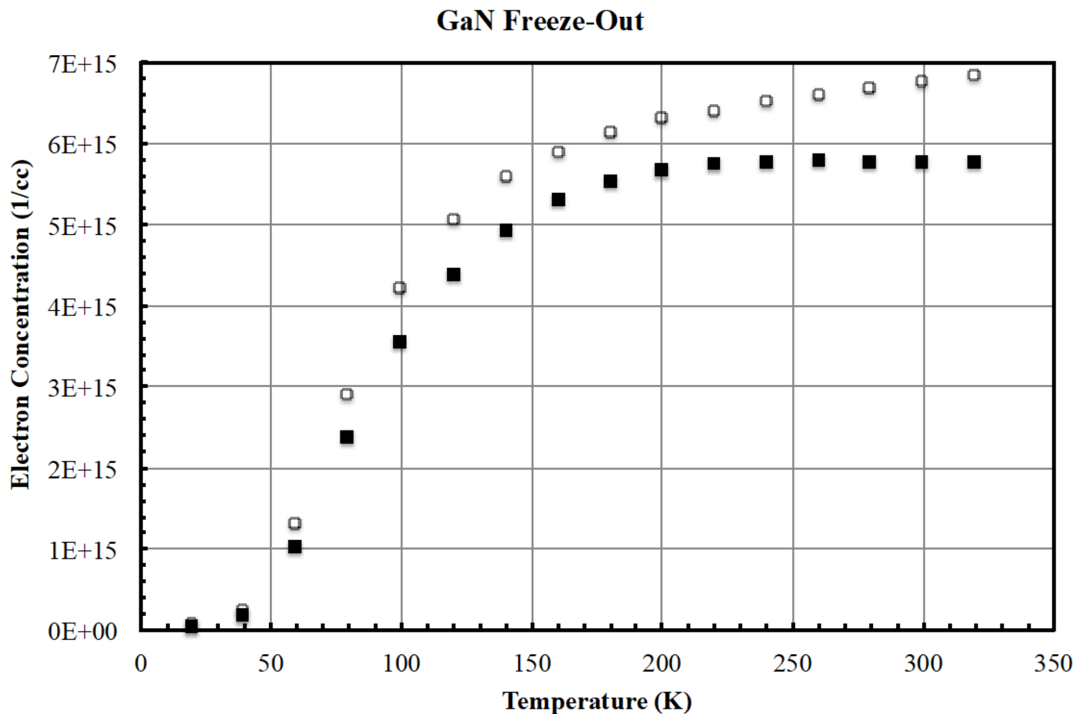

Figure 7: The Lower Data Points Show the Hall Electron Concentration Measured for Sample S703 at 2kG Magnetic Field

DISTRIBUTION STATEMENT A. Approved for public release. Distribution is unlimited.

The upper points are corrected for the Hall Factor calculated by SETA and they represent the conduction electron concentration to be analyzed below for freeze-out behavior.

The freeze-out analysis of Sample S703 is shown in Figures 8 and 9. The best-fit freeze-out curve is based on one shallow donor and one deep donor, with concentrations 6.6×10^{15} and 7.5×10^{14}/cc, and ionizations energies 31 and 155 mV. There are no acceptors. The shallow donor is typically seen, and is thought to be due to Si or O impurities. Korotkov and Wessels reported that oxygen is a simple donor in GaN and the donor activation energy is around 27 mV.[26] In Fig. 9, it is pretty clear that there is something anomalous about the lowest temperature data. An electrically conducting shunt path or lack of compliance voltage could cause this behavior since the reduced Hall Effect current would give a reduced Hall voltage and an excessive computed carrier concentration, but the actual explanation is unknown at this time. Also, the suggestion of a deep donor is certainly odd; it has no explanation at this time.

Freeze-out analysis of this sample by Look and Sizelove[12] gave the shallow and deep donor concentrations as 6.7×10^{15} and 1.7×10^{15}/cc, with acceptor concentration 1.7×10^{15}/cc, and ionization energies 26 and 50 mV. These parameters give agreement (using the present calculation method) with experiment within about 10%, indicating that the sensitivity of freeze-out analysis is not as great as one might have wished. Later, the acceptor concentration will be adjusted for a comparison between theory and experiment on Hall mobility. Lastly, one finds that using 7.6×10^{15} (29 mV) and 7.5×10^{14}/cc (155 mV) donors, and 1.0×10^{15}/cc acceptors also gives nearly as good a fit, within a few percent. So, it seems impossible to say definitively whether the acceptor concentration is zero, 1.0×10^{15}/cc, or 1.7×10^{15}/cc.

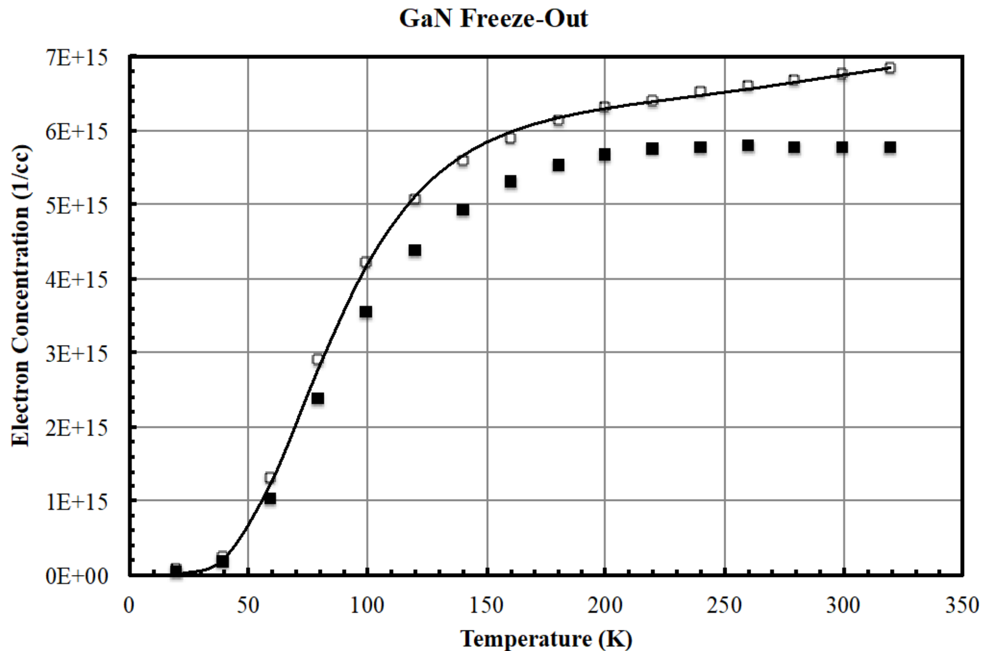

Figure 8: Same Data Points as Figure 7

The freeze-out behavior is described by the best-fit curve using one shallow donor and one deep donor, with concentrations 6.6×10^{15} and 7.5×10^{14}/cc, and ionizations energies 31 and 155mV. There are no acceptors.

DISTRIBUTION STATEMENT A. Approved for public release. Distribution is unlimited.

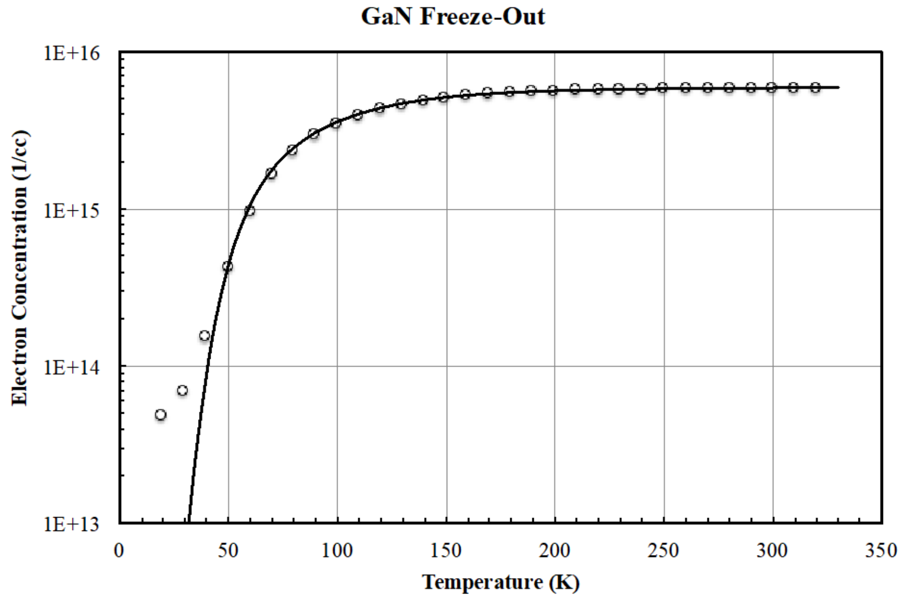

Figure 9: Same as Figure 8

Plotted with electron concentration on a logarithmic scale. Notice the spurious data at the lowest temperatures. Experiment shows proper freeze-out behavior extending over a range of a factor of 14. Several orders of magnitude would be preferable.

b) UCSB Sample 1E5

Experimental data for the high-purity n-type Gallium Nitride (GaN) Sample 1E5 provided by UCSB are shown in Figures 10, 11, and 12. The data on Hall electron concentration are shown in Figure 10, along with the Hall factor correction, which gives the conduction electron concentration shown as the upper data points. Proper freeze-out behavior extends over a range of a factor of 4000. Therefore, it is possible to accurately estimate the donor and acceptor concentrations and ionization energy using carrier freeze-out analysis.

The solid curve shown in Figsures 11 and 12 is calculated using donor and acceptor concentrations of $1.17\text{x}10^{16}$ and $1.4 \text{ x } 10^{15}$/cc and donor ionization energy 24 mV. There is no need to invoke the presence of deep donors. This result is to be contrasted with Sample S703 where there seem to be no acceptors, but there are deep donors.

Alternatively, an equally good fit to the experimental data in Figures 11 and 12 can be achieved using donor and acceptor concentrations of $1.10\text{x}10^{16}$ and $7.0 \text{ x } 10^{14}$/cc and donor ionization energy 25 mV , or donor and acceptor concentrations of $1.07\text{x}10^{16}$ and $4.0 \text{ x } 10^{14}$/cc and donor ionization energy 26 mV. So, it is difficult to say whether the compensation ratio N_a/N_d is 0.12 or 0.06 or 0.04 for this sample, based on freeze-out analysis. But, we will see something quite different when mobility is considered.

Note especially the extension of the freeze-out data all the way down to an electron concentration of $2.4 \text{ x } 10^{12}$/cc. Impressive, indeed.

DISTRIBUTION STATEMENT A. Approved for public release. Distribution is unlimited.

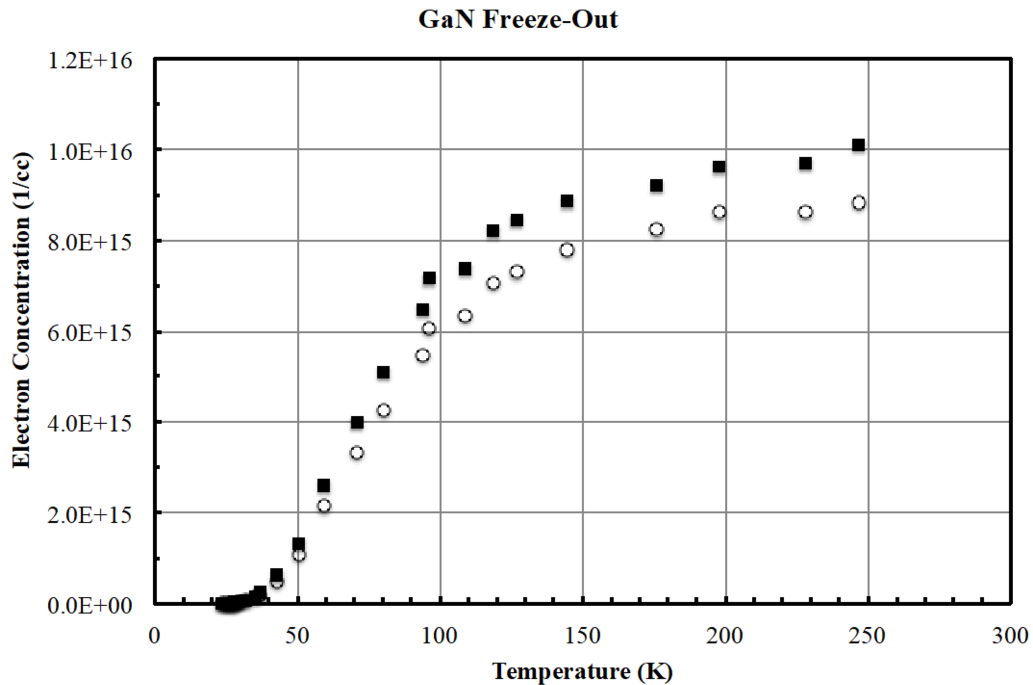

Figure 10: The Lower Data Points show the Hall Electron Concentration Measured for Sample 1E5 at 10kG Magnetic Field

The upper points are corrected for the Hall Factor and, thus, represent the conduction electron concentration.

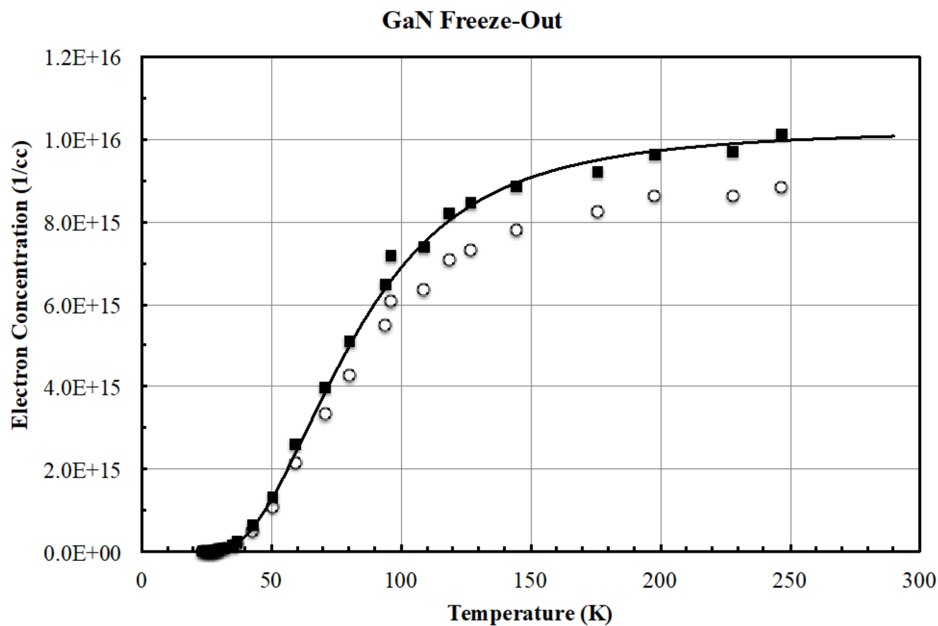

Figure 11: The Freeze-out Behavior is Described Using One Shallow Donor and One Acceptor, with Concentrations 1.17×10^{16} and 1.4×10^{15}/cc and Ionization Energy 24 mV

There are no deep donors.

DISTRIBUTION STATEMENT A. Approved for public release. Distribution is unlimited.

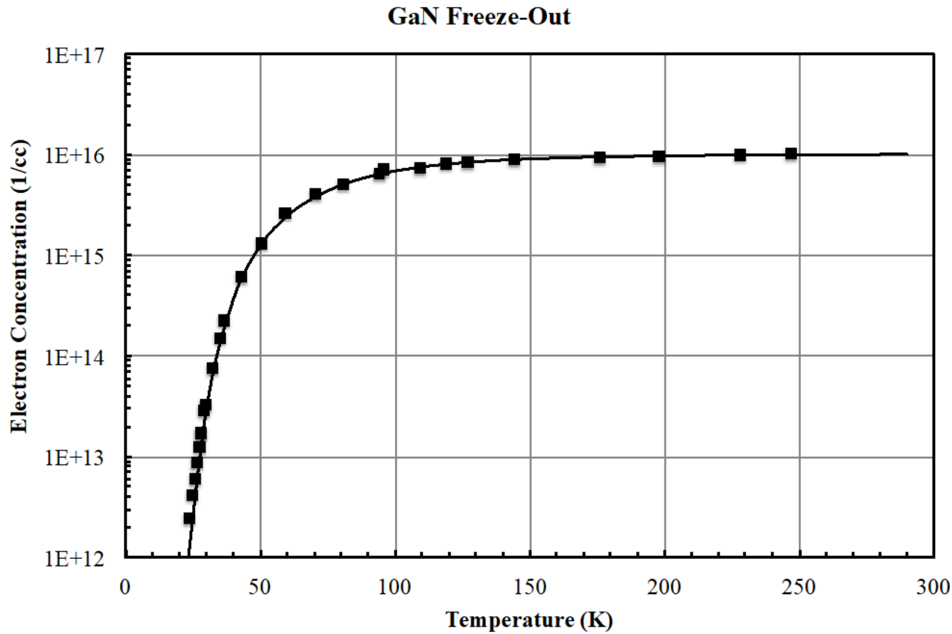

Figure 12: Same as Figure 11

Plotted with electron concentration on a logarithmic scale.

1.6 GaN Electron Mobility

"We must content ourselves with what offers the fewest disagreements." — Justin Winsor (1891)

a) AFRL Sample S703

The experimental and calculated electron Hall mobility is shown in Fig. 13 for Sample S703 for T=20 to 320K. The theoretical calculations shown by the curve are SETA calculations using the above GaN material parameters, with m* set equal to 0.22m. For both the experiment and the theoretical calculations the magnetic field is 2kG. The conduction electron concentration is given in Fig. 8 and the donor concentration is $7.35\text{x}10^{15}$/cc, as given by freeze-out analysis. The acceptor concentration is zero, *i.e.* no dopant compensation. As can be seen, the theoretical curve is about 15% too high at the highest temperatures, and it disagrees significantly with experiment at low temperatures.

In Fig. 14 the dashed curve represents the SETA calculation with donor and acceptor concentrations $8.35\text{x}10^{15}$/ and $1.0\text{x}10^{15}$/cc. Dopant compensation helps somewhat, but agreement between theory and experiment continues to be poor, relative to the 5% criterion. This is especially true for the lowest temperatures.

The logarithmic plot in Figure 15 shows the discrepancy more clearly at the highest temperatures where the disagreement is about 18%. At the lowest temperature it is about 58%. Between 100K and 260K, the agreement is more or less satisfactory, suggesting that polar-mode scattering is correctly accounted for.

DISTRIBUTION STATEMENT A. Approved for public release. Distribution is unlimited.

In any case, it is clear that dopant compensation cannot bring about satisfactory agreement between theory and experiment. This remains an open question for the data taken on Sample S703.

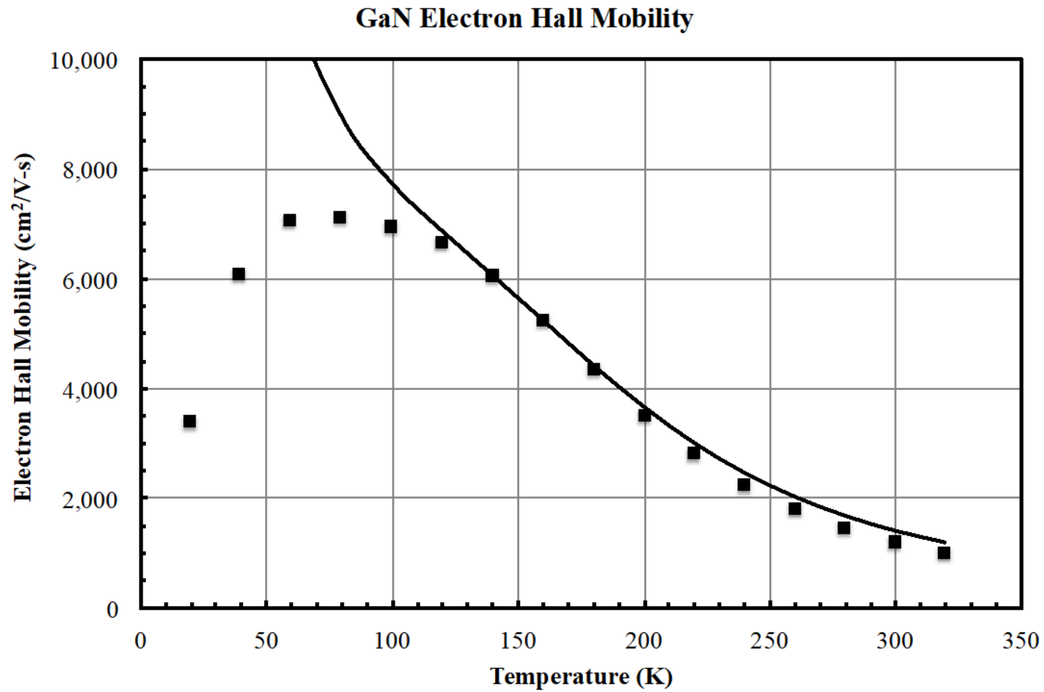

Figure 13: The Electron Hall mobility of Sample S703 is plotted, Comparing SETA Theory (curve) and Experiment (points)

The SETA donor concentration is 7.35×10^{15}/cc. Compare Figs. 8 and 9 where the total donor concentration is also 7.35×10^{15}/cc. No acceptors are assumed.

DISTRIBUTION STATEMENT A. Approved for public release. Distribution is unlimited.

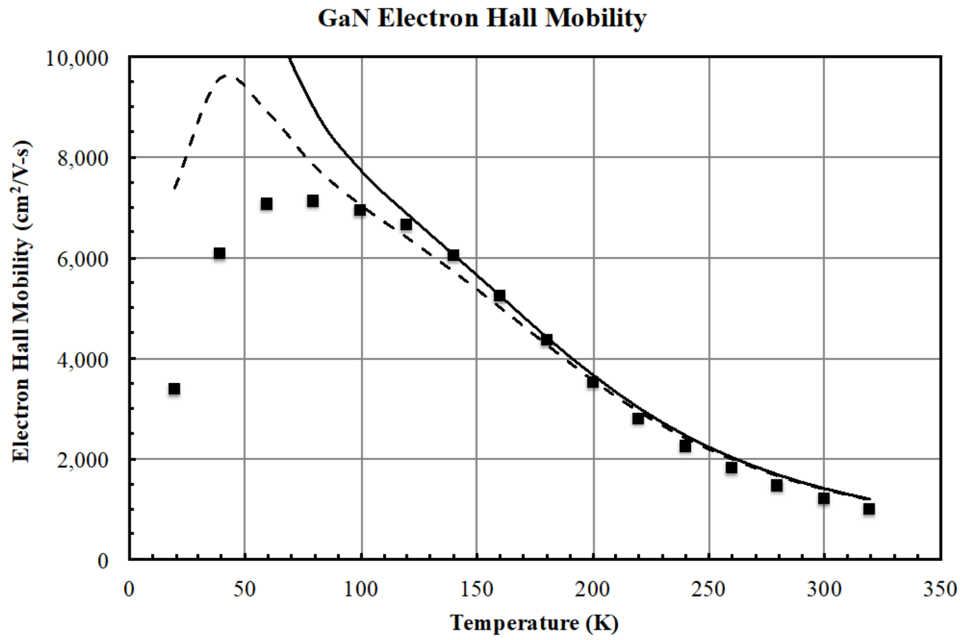

Figure 14: The Dashed Curve, the SETA Donor and Acceptor Concentrations are $8.35x10^{15}$/ and $1.0x10^{15}$/cc

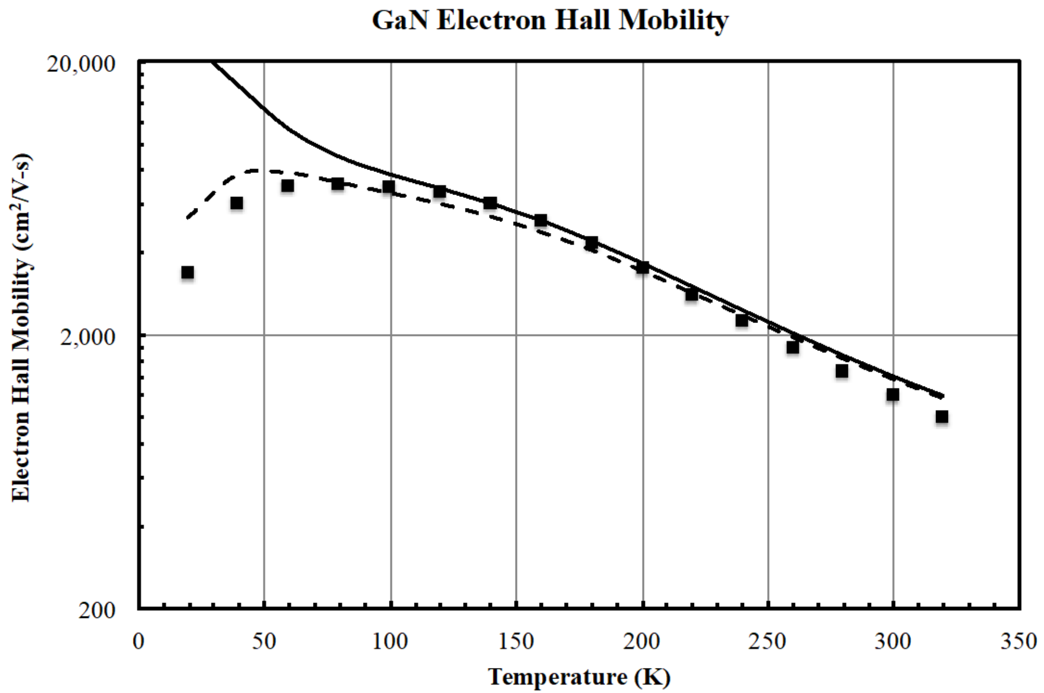

Figure 15: Same as Figure 14

Showing the error more clearly at the highest temperatures.

b) UCSB Sample 1E5

DISTRIBUTION STATEMENT A. Approved for public release. Distribution is unlimited.

The experimental and calculated electron Hall mobility is shown in Figure 16 for Sample 1E5 for T=25 to 274K. The SETA calculations are shown by the curve. For both the experiment and the theoretical calculations the magnetic field is 10kG. The conduction electron concentration is given in Fig. 11 and the donor and acceptor concentrations are $1.17x10^{16}$/cc and $1.4x10^{15}$/cc, similar to Figure 11 and 12. It can be seen that the theoretical curve is about 15% too high at the highest temperature, and 33% at the lowest temperature.

Decreasing (or increasing) the acceptor compensation as shown in Figure 17 is no panacea. It appears that the acceptor concentration must be much closer to $1.4x10^{15}$/cc than to $4.0x10^{14}$/cc, *i.e.* a compensation ratio N_a/N_d = 0.12. This result is essentially identical to that for Sample S703, *i.e.* N_a/N_d = 0.12 in Figure 14.

Figure 18 shows the results plotted on a logarithmic scale where the discrepancies can be seen more clearly. There remain serious questions about the lowest and highest temperature results and the disagreement with theory. However, it is not at all clear which may be to blame, based on these results.

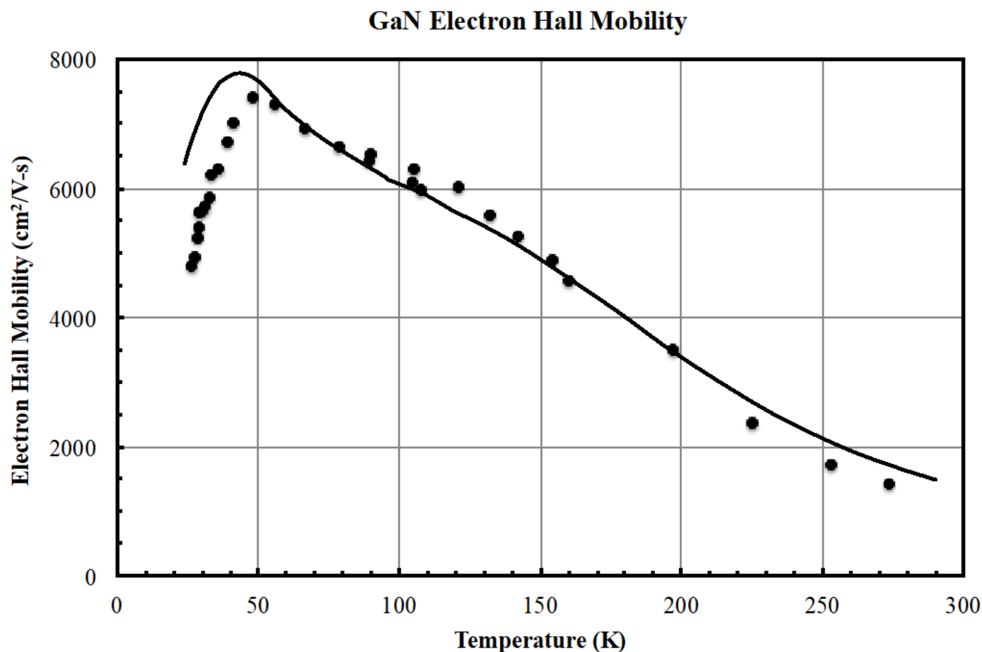

Figure 16: The Electron Hall Mobility of Sample 1E5 is Plotted, Comparing SETA Theory (curve) and Experiment (points)

The SETA donor and acceptor concentrations are $1.17x10^{16}$/cc and $1.4x10^{15}$/cc, similar to Fig. 11.

DISTRIBUTION STATEMENT A. Approved for public release. Distribution is unlimited.

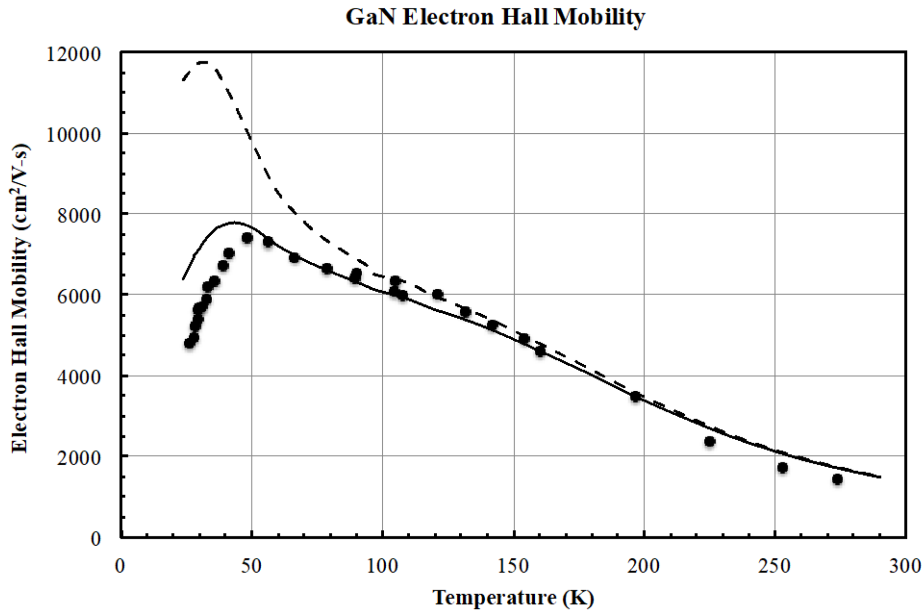

Figure 17: Electron Hall Mobility of Sample 1E5

The dashed curve, the donor and acceptor concentrations are 1.07×10^{16}/cc and 4.0×10^{14}/cc.

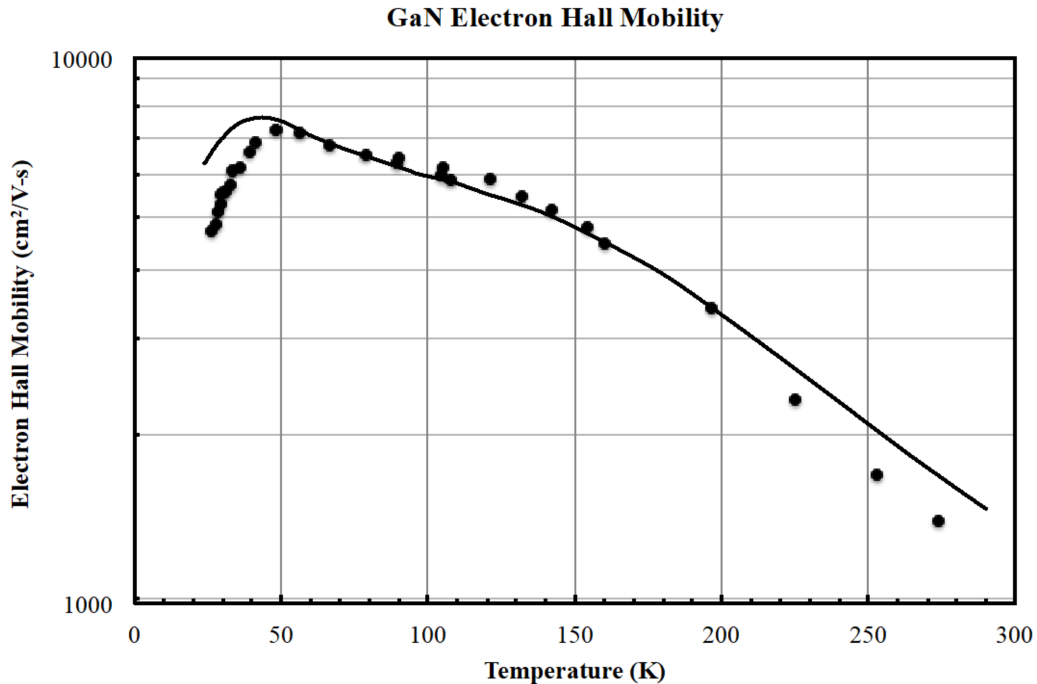

Figure 18: Same as Figure 16 on a Logarithmic Scale

Notice the discrepancies at the highest and lowest temperatures. The discrepancies between theory and experiment reach up to 15 and 33% at the highest and lowest temperatures, but may be worse outside this temperature range.

DISTRIBUTION STATEMENT A. Approved for public release. Distribution is unlimited.

c) Doped GaN

In the earlier parts of this work, a thorough examination of the doping dependence of the room-temperature electron mobility of Gallium Arsenide (GaAs) was presented. The work showed satisfactory agreement between theory and experiment, using the revised theory of ionized-impurity scattering. It also showed relatively poor agreement with the Brooks-Herring theory.

We now come full circle and do the same for GaN. Figure 19 presents experimental data by Kyle *et al.* on doped GaN. The doping level is degenerate above 2×10^{19}/cc and non-degenerate below 2×10^{18}/cc. The curve is the SETA result assuming no compensation. Although Figures 16 and 17 do indicate some acceptor compensation, the effect on 296K mobility is insignificant at the relatively low acceptor concentrations 1.4×10^{15}/cc and 4.0×10^{14}/cc shown there.

Agreement is satisfactory for the two highest doped and the one lowest doped samples. Little can be said regarding the remaining three. The same results are plotted on a logarithmic scale in Figure 20 and compared to the Brooks-Herring theory (dashed curve). As expected, both theories are similar for low doping, below 2.0×10^{17}/cc, but they disagree significantly for degenerate material, as was also seen in the earlier work on GaAs. If one were to explain the results using the BH theory in conjunction with acceptor compensation, the compensating acceptor concentration would need to lie in the 10^{19}/cc range.

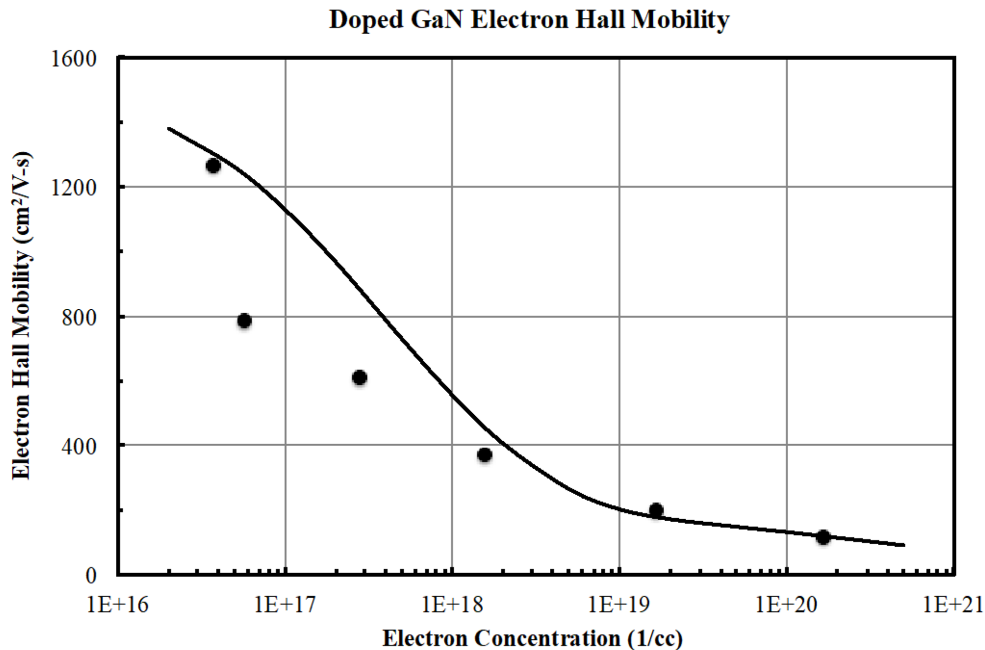

Figure 19: Electron Hall Mobility of Doped n-type GaN

Experiment (points) is compared to theory (curve) assuming no acceptor compensation. T=296K and B=10kG.

DISTRIBUTION STATEMENT A. Approved for public release. Distribution is unlimited.

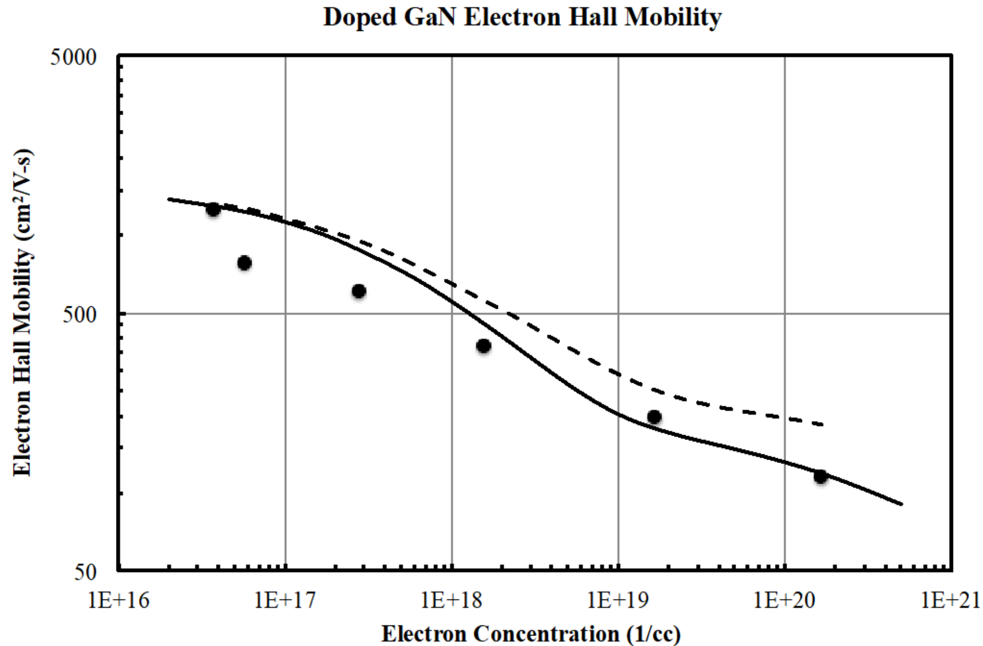

Figure 20: Same as Figure 19

Comparing Brooks-Herring scattering (dashed curve) to revised theory (solid curve) assuming no acceptor compensation.

1.7 Conclusions and Recommendations

Regarding heavily doped ZnO, the results shown in Figure 4 leave little to be desired. Agreement between the revised theory and experiment is within the desired 5% criterion. More work on high-purity material is needed to settle on correct material parameters for various temperatures.

To conclude the discussion on the electron transport properties of GaN, Figure 21 shows electron Hall mobility as a function of temperature for two high-purity GaN samples, Morkoç (open circles) and Kyle (solid circles, same as Fig. 18). Overall, the good agreement between the two experiments is striking. However, a conundrum arises at the lowest temperatures. It was shown earlier in Figs. 15 and 18 that experiment falls far below theory for low enough temperatures. This is clearly apparent for the solid circles in Fig. 21. However, and most importantly, the open circle at the very lowest temperature (25K) agrees extremely well with theory (within a fraction of one percent). But, the point at 35K falls well below the curve. So, which are we to believe?

DISTRIBUTION STATEMENT A. Approved for public release. Distribution is unlimited.

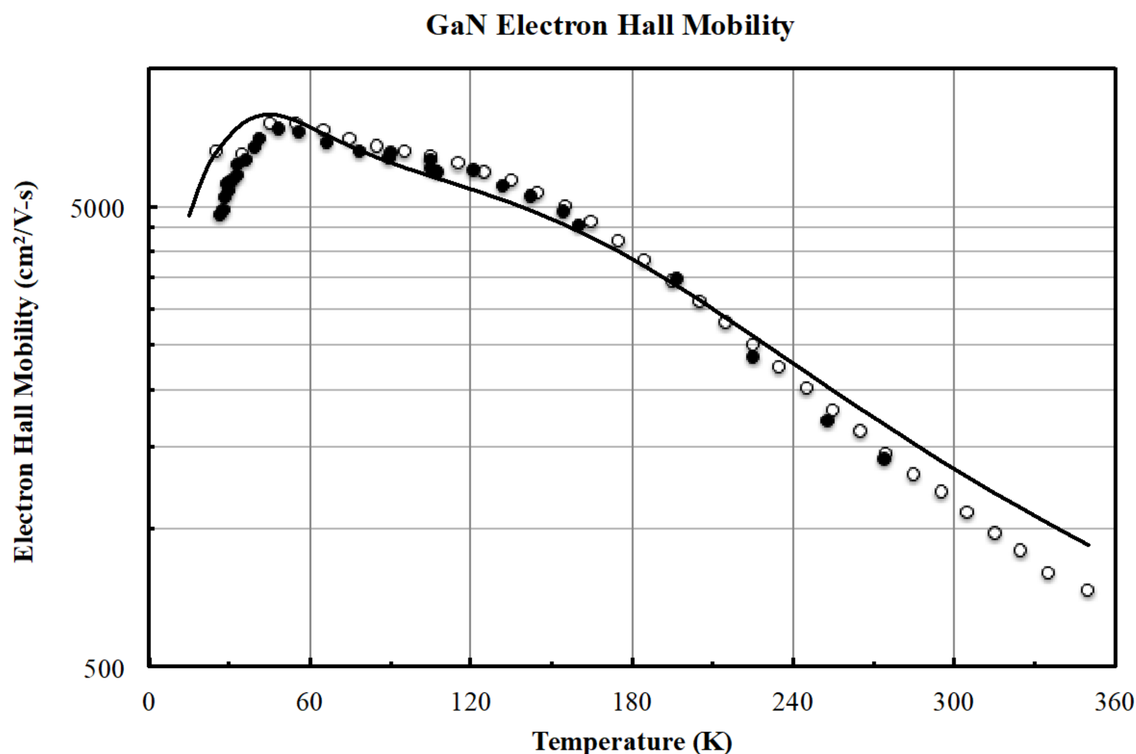

Figure 21: Data Points by Morkoç (open circles) and Kyle (solid circles)
The SETA donor and acceptor concentrations are $1.39x10^{16}$*/cc and* $1.4x10^{15}$*/cc from the Morkoç data freeze-out analysis. Notice the disagreement at high temperature and the peculiar Morkoç datum at 35K; or is the 25K datum peculiar?*

It is also evident that the high-temperature discrepancy remains. It would helpful to have experiments carried out up to 1000K. Tokuda *et al.*[27] have made measurements up to 1020K but the results appear to be anomalous, resulting in a novel interpretation.

One recommendation regarding Hall Effect measurements: it should always be required that low-doped samples which show freeze-out should exhibit Hall electron concentrations spanning a range of at least three orders of magnitude, *i.e.* at least 1000:1. The samples in Figure 21 show ranges of 4000:1 (Kyle) and 10,600:1 (Morkoç) while Fig. 9 shows merely 14:1. It is difficult to see how the low-temperature value of Hall mobility would be impacted in the latter case, but it is suspicious.

In conclusion, it appears that the revised theory of ionized-impurity scattering is capable of explaining experimental results on degenerately doped semiconductors. The situation with regard to GaAs and ZnO seems to be settled. On the other hand, GaN needs further work to construct a reliable set of basic material parameters, but the initial results are promising.

DISTRIBUTION STATEMENT A. Approved for public release. Distribution is unlimited.

2 ACKNOWLEDGMENTS

Supported by the Air Force Office of Scientific Research under Project FA9550-20RXCOR046-RY. This work would not have been possible without encouragement, support, and advice from John S. Cetnar. David C. Look (WSU), Erin Kyle and James Speck (UCSB), and Hadis Morkoç (VCU) have been extraordinarily generous with data and comments, which I most sincerely acknowledge.

DISTRIBUTION STATEMENT A. Approved for public release. Distribution is unlimited.

APPENDIX: CARRIER FREEZE-OUT

Consider n-type material where the acceptors are completely ionized and there are two donors, denoted by subscripts 1 and 2. For donors with concentration N_1 and ionization energy E_1, the ionized donor concentration is,

$$N_1^+ = \frac{N_1}{1+(g_1 n / N_C)e^{E_1/\kappa T}}$$

The donor degeneracy ratio g_1 is equal to 2; the conduction electron concentration is n; and the thermal density of states in the conduction band is N_C.

For donors with ionization energy E_2, the ionized donor concentration is,

$$N_2^+ = \frac{N_2}{1+(g_2 n / N_C)e^{E_2/\kappa T}}$$

The donor degeneracy ratio g_2 is equal to 2. Acceptors with concentration N_a are assumed to be completely ionized.

$$N_a^- = N_a$$

Ignoring minority carriers and combining equations by means of the charge neutrality equation gives,

$$n + N_a^- = N_1^+ + N_2^+$$

The electron concentration n can be expressed as an implicit quadratic equation, which can be solved by iteration. Because the electron concentration is also expressed in terms of the Fermi Level, it is easier to solve for the Fermi Level and to calculate n from that.

$$n = N_C e^{E_F/\kappa T}$$

For convenience, introduce the following notation.

$$x = e^{E_F/\kappa T}$$

$$D_1 = g_1 e^{E_1/\kappa T}$$

$$D_2 = g_2 e^{E_2/\kappa T}$$

So,

$$n = N_C x$$

The charge neutrality equation gives,

$$N_C x + N_a = \frac{N_1}{1+D_1 x} + \frac{N_2}{1+D_2 x}$$

Or

$$N_C x + \left(N_a - \frac{N_2}{1+D_2 x} \right) = \frac{N_1}{1+D_1 x}$$

Thus, we have the quadratic equation, implicit in x and n.

$$D_1 N_C x^2 + N_C x + D_1 \left(N_a - \frac{N_2}{1+D_2 x} \right) x + \left(N_a - \frac{N_2}{1+D_2 x} \right) - N_1 = 0$$

DISTRIBUTION STATEMENT A. Approved for public release. Distribution is unlimited.

The solution for x and, hence, n is

$$x = e^{E_F/\kappa T} = -\frac{N_C + D_1\left(N_a - \frac{N_2}{1+D_2 x}\right)}{2D_1 N_C} + \sqrt{\left[\frac{N_C + D_1\left(N_a - \frac{N_2}{1+D_2 x}\right)}{2D_1 N_C}\right]^2 + \frac{N_1 - N_a + \frac{N_2}{1+D_2 x}}{D_1 N_C}}$$

Obviously, additional donors can be accommodated by adding more donor terms after each of the N_2 terms. This equation can be solved by iteration. To see that it is a contraction mapping, and therefore that it has a unique solution, and that an iterative sequence will converge to a "fixed point," consider the somewhat similar cubic equation, with the obvious solution $x = 3$.

$$x^3 = 27$$

This can be written as an iterative sequence.

$$x_{i+1} = \sqrt{27/x_i}$$

Starting from $x_0 = 1$, the sequence converges to the solution within 1% in 7 iterations as shown here.

1	5.196152423
5.196152423	2.279507057
2.279507057	3.441608071
3.441608071	2.800923042
2.800923042	3.104783301
3.104783301	2.948942029
2.948942029	3.025859542
3.025859542	2.987153223
2.987153223	3.006444093
3.006444093	2.996783135
2.996783135	3.001609727

To prove that this is a contraction mapping, one must prove that $\theta < 1$ for the following.

$$\left|\sqrt{27/x_i} - \sqrt{27/x_{i+1}}\right| = \theta\left|x_i - x_{i+1}\right|$$

$$\left|\sqrt{27/x_i} - \sqrt{27/\sqrt{27/x_i}}\right| = \theta\left|x_i - \sqrt{27/x_i}\right|$$

$$\left|\sqrt{27} - 27^{1/4} x_i^{3/4}\right| = \theta\left|x_i^{3/2} - \sqrt{27}\right|$$

$$\left|3^{3/2} - (3x_i)^{3/4}\right| = \theta\left|x_i^{3/2} - 3^{3/2}\right|$$

$$\therefore \theta < 1 \ \textit{provided} \ x_i > 0 \ \textit{and} \neq 3$$

DISTRIBUTION STATEMENT A. Approved for public release. Distribution is unlimited.

3 REFERENCES

1. Final Report, Phase 1, Prime Contract: FA9550-20RXCOR046-RY
2. Final Report, Phase 2, Prime Contract: FA9550-20RXCOR046-RY
3. J. S. Cetnar personal communication
4. J. S. Cetnar and D. L. Rode, Journal of Electronic Materials **48**, 3399 (2019) is used to confirm Fermi Level and screening length computations
5. D. L. Rode, Phys. Rev. **B2** (1970) 4036
6. D. L. Rode, *Semiconductors and Semimetals* **15** (Academic Press, New York, 1975)
7. D. C. Look, K. D. Leedy, L. Vines, B. G. Svensson, A. Zubiaga, F. Tuomisto, D. R. Doutt, and L. J. Brillson, Phys. Rev. **B84** (2011) 115202
8. N. Miura and Y. Imanaka Phys. Stat. Solidi b **237** (2003) 237
9. A. R. Hutson, J. Phys. Chem. Solids **8** (1959) 467
10. R. Hauschild, H. Priller, and C. Klingshirn, Phys. Stat. Sol. c (2005) 64643
11. I. Vurgaftman and J. R. Meyer, J. Appl. Phys. **94** (2003) 3675
12. D. C. Look and J. R. Sizelove, Appl. Phys. Letts. **79** (2001) 1133
13. W. Shan, T. Schmidt, X. H. Yang, J. J. Song, and B. Goldenberg, J. Appl. Phys. **79** (1996) 3691
14. A. S. Barker, Jr. and M. Ilegems Phys. Rev. **B7** (1973) 743
15. Kihoon Park , Ahmed Mohamed, Mitra Dutta, Michael A. Stroscio, and Can Bayram, Scientific Reports **8** (2018) 15947
16. H. Harima, J. Phys. Condens. Matter **14** (2002) R967
17. K. Park, K., M. A. Stroscio, and C. Bayram, J. Appl. Phys. **121** (2017) 245109
18. V. Yu. Davydov, Yu. E. Kitaev, I. N. Goncharuk, A. N. Smirnov, J. Graul, O. Semchinova, D. Uffmann, M. B. Smirnov, A. P. Mirgorodsky, and R. A. Evarestov, Phys. Rev. **B58** (1998) 12 899
19. A. Polian, M. Grimsditch, and I. Grzegory, J. Appl. Phys. **79** (1996) 3343
20. V. A. Savastenko and A. U. Shelag, Phys. Stat. Sol. A **48** (1978) K135
21. P. Perlin, E. Litwin-Staszewska, B. Suchanek, W. Knap, J. Camassel, T. Suski, R. Piotrzkowski, I. Grzegory, S. Porowski, E. Kaminska, J. C. Chervin, Appl. Phys. Letts. **68** (1996) 1114
22. D. Huang, F. Yun, M. A. Reshchikov, D. Wang, H. Morkoç, D. L. Rode, L. A. Farina, C. B. Kurdak, K. T. Tsen, S. S. Park, and K. Y. Lee, Solid State Electronics **45** (2001) 711
23. D. C. Look and T. A. Cooper, personal communication
24. Erin C. H. Kyle, Stephen W. Kaun, Peter G. Burke, Feng Wu, Yuh-Renn Wu, and James S. Speck, J. Appl. Phys. **115** (2014) 193702 and personal communication
25. H. Morkoç, personal communication
26. cited in J. K. Sheu and G. C. Chi, J. Phys. Condens. Matter **14** (2002) R657
27. H. Tokuda, K. Kodama, and M. Kuzuhara, Appl. Phys. Letts. **96** (2010) 252103

DISTRIBUTION STATEMENT A. Approved for public release. Distribution is unlimited.

LIST OF SYMBOLS, ABBREVIATIONS, AND ACRONYMS

ACRONYM	DESCRIPTION
AFRL	Air Force Research Laboratory
BH	Brook-Herring
GaAs	Gallium Arsenide
GaN	Gallium Nitride
SETA	Semiconductor Electronic Transport Analysis
ZnO	Zinc Oxide

DISTRIBUTION STATEMENT A. Approved for public release. Distribution is unlimited.